(average 2.87 Å) and a larger Ru-Ru distance of 3.15 Å. The Ru···Ru distance in **5e** is also to be compared to the PPh_2-bridged ruthenium atom distances of 3.147 (1) and 3.171 (1) Å while the Ru-Ru bond length is 3.098 (1) Å in $FeRu_3(CO)_{13}(\mu\text{-}PPh_2)_2$.[25]

Actually the $FeRu_2(\mu\text{-}Cl)_2$ arrangement in **5e** can be compared directly to the $RuCl_3Ru$ moiety in $Cl_3Sn(CO)_2RuCl_3Ru(CO)_3$[26] by formal displacement of *one* bridging chlorine atom by the $Fe(CO)_4$ group; indeed for this compound the average Ru-Cl distance is 2.44 Å [2.465 (5) Å for **5e**] with a Ru(1)-Cl-Ru(2) angle of 80.7 (4)° [80.7 (2)° for **5e**].

The coordination around the three metal atoms in such that the $FeRu_2Cl_2(CO)_8P_2$ skeleton has approximate C_{2v} symmetry. Both phosphorous atoms lie slightly out of the $FeRu_2$ plane and are unsymmetrically located with respect to the Fe, Cl(1), Cl(2) plane (Table S1). The ruthenium atoms have a distorted octahedral stereochemistry, but the distorsions are similar to that found in $Cl_3Sn(CO)_2RuCl_3Ru(CO)_3$.[26]

The Fe-Ru(1)-P(1) and Fe-Ru(2)-P(2) angles are significantly different: 176.1 (1) and 174.3 (1)°, respectively. The Fe-Ru(1)-C(6) angle [87.2 (4)°] also differs significantly from the Fe-Ru(2)-C(8) angle [92.3 (4)°]. These angular differences may be due to intermolecular steric interaction between $Ph_2PC{\equiv}C\text{-}t\text{-}Bu$ ligands of different molecules in the solid state as shown by the short intermolecular distances (Table S2). The bonds within the ligands $Ph_2PC{\equiv}C\text{-}t\text{-}Bu$ do not show any particularities; the $PC{\equiv}CC$ chains are roughly linear 174 (2)° and 177 (1)° with a $C{\equiv}C$ bond length of 1.19 (4) Å. The most interesting aspect is the relative positions of the alkyne chains which destroy the C_{2v} symmetry: one is above the $FeRu_2$ plane making an angle of 23° and the other one underneath with an angle of 33°. Moreover the angle between the alkyne chains is 102°, and their relative orientations minimize the interactions between the phenyl groups and the two ligands. These relative positions of the phosphinoalkyne ligands may be responsible for the slight difference between the ruthenium-phosphorus bond lengths [Ru(1)-P(1) = 2.374 (5) Å and Ru(2)-P(2) = 2.383 (5) Å]. Finally, it should be pointed out that there may be a relationship between the reactivity of a coordinated phosphinoalkyne in a polymetallic complex and its relative position with respect to a metal-metal bond. The derivative $Ru_3(CO)_9(Ph_2PC{\equiv}C\text{-}t\text{-}Bu)_3$ for which the phosphinoalkyne ligands lie in a cis position with respect to the Ru-Ru bond[19] undergoes oxidative cleavage of phosphorus-carbon(alkyne) bond affording $Ru_3(CO)_6(\mu\text{-}C_2\text{-}t\text{-}Bu)(\mu\text{-}\eta^2\text{-}C_2\text{-}t\text{-}Bu)(\mu\text{-}PPh_2)_2(Ph_2PC_2\text{-}t\text{-}Bu)$.[27] By contrast for compound **5e** such a behavior was not observed. The inhibition to oxidative cleavage may be due to the presence of chloro bridges but also to the trans position of the phosphinoalkynes with respect to the Fe-Ru bonds.

Acknowledgment. The authors are grateful to Professor A. J. Carty for helpful discussions and D.F.J. thanks the DGRST for the award of a studentship.

Registry No. **1a**, 35796-50-0; **1b**, 39732-57-5; **1c**, 39732-59-7; **1d**, 67612-85-5; **1e**, 77187-27-0; **2a**, 78168-08-8; **2d**, 77187-28-1; **3a**, 78168-09-9; **3b**, 77187-30-5; **3c**, 78168-10-2; **3d**, 77187-29-2; **4a**, 78168-11-3; **4b**, 77308-83-9; **4c**, 78168-12-4; **4d**, 77308-84-0; **5a**, 78168-13-5; **5b**, 77187-25-8; **5c**, 78168-14-6; **5d**, 77187-24-7; **5e**, 77187-26-9; **9**, 78168-15-7; $Fe_2(CO)_9$, 15321-51-4.

Supplementary Material Available: A listing of observed and calculated structure factor amplitudes, Table S1 (least-squares planes and atomic displacement therefrom), Table S2 (intramolecular interactions), and Figure S1 (unit cell packing) (13 pages). Ordering information is given on any current masthead page.

(25) Churchill, M. R.; Bueno, C.; Young, D. A., personal communication.
(26) Elder, M.; Hall, D. *J. Chem. Soc. A* **1970**, 245.
(27) Carty, A. J.; Taylor, N. J.; Smith, W. F. *J. Chem. Soc., Chem. Commun.* **1979**, 750.

Contribution from Laboratoire CNRS-SNPE, 94320 Thiais, France, and Laboratoire de Cristallochimie, Institut Le Bel, Université Louis Pasteur, 67070 Strasbourg Cedex, France

Reaction of Lithium Alkyls and Aryls with 1,1'-Diphosphaferrocenes. Synthesis and Structure of a Stable Bis(diene)iron(-I) Species

BERNARD DESCHAMPS,[1a] JEAN FISCHER,[1b] FRANÇOIS MATHEY,*[1a] and ANDRÉ MITSCHLER[1b]

Received January 20, 1981

The reaction of 2 equiv of alkyllithium and 3 equiv of alkyl halide with 1,1'-diphosphaferrocene yields a stable green paramagnetic bis(η^4-phospholium)iron halide in which iron bears formally 17 electrons. The stability of these species increases with the bulkiness of the alkyl chains. The product with *tert*-butyl and methyl P substituents was studied by X-ray. The two most striking characteristics of its structure are the absence of a phosphorus-iron bond and the impressive folding of the phospholium nucleus around the Cα-Cα' axis ($\simeq$31°). Crystal data for $FeP_2IC_{22}H_{40}$ are a = 10.640 (1) Å, b = 10.865 (2) Å, c = 24.908 (4) Å, α = 90.14 (1)°, β = 95.06 (1)°, γ = 112.24 (1)°, V = 2653 Å^3, Z = 4, d_{calcd} = 1.37 g cm^{-3}, and space group $P\bar{1}$. The mechanism of formation of these products probably includes the nucleophilic attack of alkyllithium onto one of the phosphorus atoms of 1,1'-diphosphaferrocene followed by the electrophilic attack of the alkyl halide onto the same phosphorus giving a transient (phospholium)(phospholyl)iron species. When phenyllithium was used, this transient species was spontaneously oxidized and gave a stable (η^4-phospholium)(η^5-1-hydroxy-1-oxophospholato)iron diamagnetic zwitterion, the structure of which was also established by X-ray. The existence of such a compound demonstrates that the phosphole P(O)OH acids are able to chelate a metal between their phosphinate function and their dienic system. Crystal data for $FeP_2O_3C_{19}H_{26}$ are a = 9.822 (1) Å, b = 9.845 (1) Å, c = 10.913 (1) Å, α = 74.64 (1)°, β = 67.02 (1)°, γ = 80.74 (1)°, V = 935 Å^3, Z = 2, d_{calcd} = 1.49 g cm^{-3}, and space group $P\bar{1}$.

From all the data gathered up to now, it appears that the phosphorus atom of phosphametallocenes **1** has, broadly speaking, lost its classical nucleophilicity and, conversely, acquired some electrophilicity as is the case with phosphorins **2**.[2]

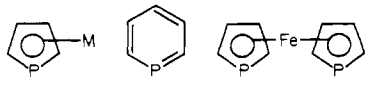

1 2 3

(1) (a) Laboratoire CNRS-SNPE. (b) Institut Le Bel.
(2) K. Dimroth, *Top. Curr. Chem.*, **38**, 20 (1973); G. Märkl, *Phosphorus Sulfur*, **3**, 77 (1977); A. J. Ashe III, *Acc. Chem. Res.*, **11**, 153 (1978).

0020-1669/81/1320-3252$01.25/0

A theoretical study of phosphacymantrenes[3] (**1**, M = Mn(CO)$_3$) has shed some light on this question. In usual P^{III} compounds, the lone pair orbital is also the HOMO whereas in unsubstituted phosphacymantrene, it is only the fourth highest occupied orbital. Conversely, the LUMO is primarily localized on the phosphorus atom in the latter case. As a result, the electrophilicity of phosphacymantrenes is so high that they are destroyed even by sodium cyanide in alcohol.[4] In the case of 1,1′-diphosphaferrocenes (**3**), however, the electrophilicity of phosphorus has decreased to such a level that they are not destroyed any more by nucleophilic media,[5] and, thus, the isolation of complexes resulting from nucleophilic attacks at phosphorus becomes conceivable. With this hope in mind, we decided to study the reaction of lithium alkyls and aryls with 1,1′-diphosphaferrocenes. We have just shown previously[5] that *n*-butyllithium does not metalate the α-CH of these species as would be the case if they behaved as ferrocenes or classical aromatic heterocycles.

Results and Discussion

Synthesis. All our work has been performed with readily available 3,3′,4,4′-tetramethyl-1,1′-diphosphaferrocene (**4**).[5] As a first step we decided to investigate, by ^{31}P NMR at −80 °C in THF, the reaction of *t*-BuLi with **4**. The addition of 1 equiv of *t*-BuLi to the solution of **4** led to the complete disappearance of the ^{31}P signal at −72 ppm (reference H_3PO_4, δ positive for downfield shifts), which is associated with **4**, and to the appearance of two new broad signals at −21.8 and −95.4 ppm. The most logical explanation is to admit that reaction 1 has taken place (similar reactions are encountered with phosphorins[2]).

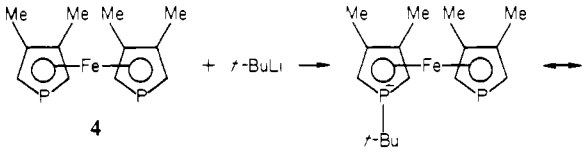

4 5A

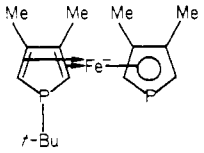

5B (1)

The signals at −95.4 and −21.8 ppm are respectively associated with the phospholyl and the *tert*-butylphosphole of **5**. The fact that the phospholyl signal is notably shielded by comparison with that of **4** and that the phosphole signal appears in the region normally associated with phosphines indicates that the structure of **5** is probably closer to **5B** than to **5A**. The further addition of 1, 2, or 3 equiv more of *t*-BuLi to the solution brings no significant change to the ^{31}P spectrum (a slight shift is observed on the high-field signal from −95.4 to −102.4 ppm). The phospholyl of **5** seems to have lost its electrophilicity and this again suggests that iron bears a strong negative charge.

We then attempted to trap the postulated anionic species. The addition to the THF solution of **4** of 1 equiv of *t*-BuLi followed by 1 equiv of IMe led only to the recovery of **4** itself. A possible explanation lies in the spontaneous decomposition of the expected complex **6** by a reaction similar to the thermal conversion of λ^5-phosphorins into λ^3-phosphorins, which, however, occurs at much higher temperatures (~200–300 °C).[2]

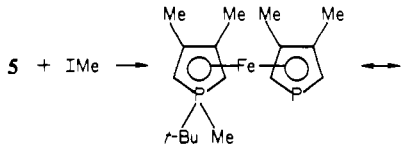

6A

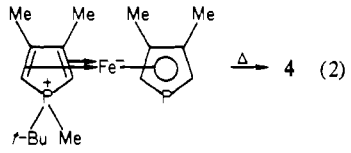

6B

In spite of this discouraging result, we continued our experiments and discovered that, if at least 2 equiv of *t*-BuLi and 3 equiv of IMe were added to the THF solution of **4** at −80 °C, then it was possible to isolate by chromatography a stable, water-soluble, paramagnetic, green monocation **7** to which a bis(η^4-diene)iron structure was attributed on the basis of the X-ray data (see hereafter).

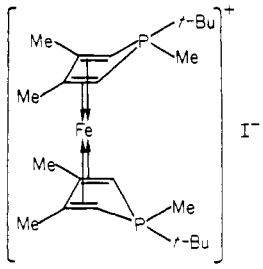

7

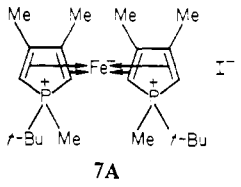

7A

Indeed the very long P···Fe distances (~2.69 Å) preclude the existence of any kind of bonds between iron and phosphorus, and, thus, the phosphole moieties of **7** act only as η^4 ligands by their dienic systems. At least formally, then, **7** contains a 17-electron iron(−I) sandwiched between two phospholium units as depicted in formula **7A**. At this point it is interesting to note that **7** reacts readily with aqueous IH to yield the expected phospholium salt **8**:

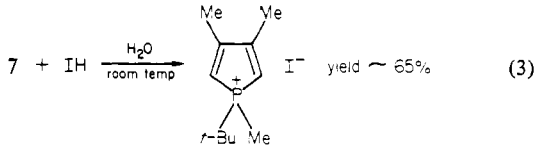

8

Of course, the stability of such an unusual arrangement is probably due to the partial delocalization of the negative charge onto the phospholium ligands. Another reason is certainly the steric bulk of the phospholium units. Indeed, when the same experiments are carried out with *n*-BuLi or MeLi, complexes **9** and **10** are isolated respectively, but it

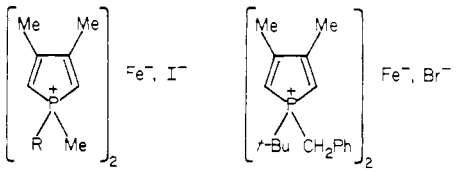

9, R = *n*-Bu
10, R = Me

13

(3) C. Guimon, G. Pfister-Guillouzo, and F. Mathey, *Nouv. J. Chim.*, 3, 725 (1979).
(4) F. Mathey, A. Mitschler, and R. Weiss, *J. Am. Chem. Soc.*, **100**, 5748 (1978).
(5) G. de Lauzon, B. Deschamps, J. Fischer, F. Mathey, and A. Mitschler, *J. Am. Chem. Soc.*, **102**, 994 (1980).

Scheme I. Possible Mechanism for the Formation of **7**

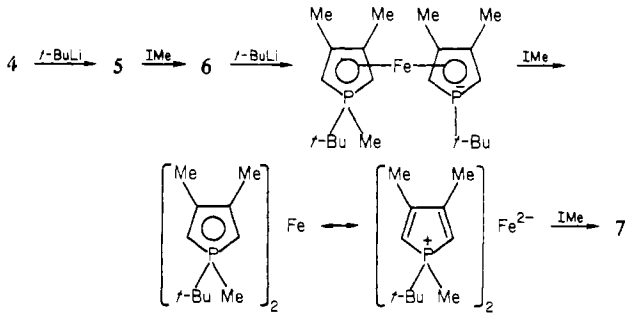

12

clearly appears that the stability and the yields decrease in the order **7 > 9 > 10**, that is, in the same order as the steric bulk of phosphorus substituents.

In view of the results of the ^{31}P NMR study reported above, a logical sequence for explaining the formation of **7** is depicted in Scheme I. The two features of this scheme are as follows: (a) The four P–C bonds form sequentially. The attack of the second phosphorus starts only after "neutralization" of the first negative charge in agreement with the ^{31}P NMR experiments. (b) IMe is reduced by **12**, which is probably a strong reducing agent in spite of its 18-electron configuration. Here it must be noted that IMe can be replaced by $PhCH_2Br$ in this sequence. Complex **13** is thus obtained, and this means, if our scheme is correct, that benzyl bromide can also act as an oxidizing agent for species such as **12**.

We then attempted to generalize this reaction by replacing *t*-BuLi by PhLi. To our surprise, it was impossible to obtain the same type of complex. On the contrary, by adding only 1 equiv of PhLi and an excess of IMe to the THF solution of **4** at −80 °C, we obtained a red covalent diamagnetic complex to which structure **14** was ascribed on the basis of the X-ray data (see hereafter).

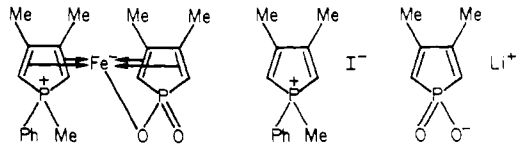

14 **15** **16**

The coordination of the phosphoryl oxygen to the iron atom is demonstrated by the value of the Fe···O distance (2.15 Å), whereas the Fe···P^+ distance (2.73 Å), similar to those found in **7**, precludes the existence of a bond between this phosphorus and the sandwiched atom. Clearly, **14** is formed by spontaneous oxidation of a transient species analogous to **6**, and, thus, we have now a strong experimental evidence in favor of the mechanism postulated in Scheme I. The spectral data of **14** are in good agreement with the X-ray structure. Thus, the ^{31}P NMR spectrum of **14** shows two singlets at 1.9 and 24.5 ppm ($CDCl_3$) to be compared with the data of the free phospholium salt **15** ($\delta(^{31}P)$ = 31.5[6]) and of the free lithium phosphinate **16** ($\delta(^{31}P)$ = 45[7]). The observed phosphorus shieldings in **14** are probably the result of the η^4 complexation of the phosphole moieties. On the other hand, the ^1H NMR spectrum (see the Experimental Section) shows clearly the existence of two inequivalent phosphole units and the IR spectrum shows a P=O band at 1208 cm^{-1} (KBr). When treated with aqueous IH, **14** gives, as expected, the phospholium salt **15** and the free acid **17**, which is unstable (eq 4).

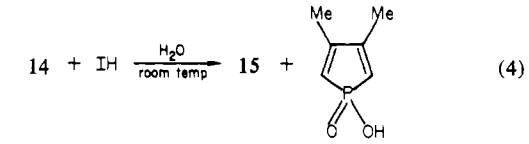

(4)

17

Finally, we want to stress one more point. In the literature, numerous η^4 complexes of phosphole oxides,[8] phosphole esters,[9] and phosphole acids[10] (similar to **17**) are described, but the discovery of **14** proves for the first time that a phosphole acid is also able to chelate a metal by acting as a five-electron ligand through its dienic system and its phosphinic group.

Crystal Structure of Complexes 7 and 14. Table I lists the crystal data for compounds **7** and **14**. Tables II and III give the atomic positional and thermal parameters with their estimated standard deviations for **7** and **14**, respectively.

7. The crystal structure of $[(CH_3)_2C_4H_2P(CH_3)(C_4H_9)]_2Fe^+$ (**7**) consists of discrete molecules in which one iron atom is sandwiched between two π-bonded phosphole rings. There are two such molecules in the asymmetric unit only linked by hydrogen bonds and van der Waals type interactions. Table IV gives the shortest intermolecular distances. Figure 1 gives a view of a molecule.[11]

Table V gives selected bond lengths (Å) and angles (deg) for each molecule with averages and esd's. Table VI gives the least-squares planes of interest and some dihedral angles.

The phosphole rings are not planar: the dihedral angles between least-squares planes C1–C4 and C1–P–C4 have a mean value of 30.9°. Consequently the mean value of the iron–phosphorus bond is greater by about 0.4 Å than that

Table I. X-ray Experimental Data

	7	**14**
compd	$FeP_2IC_{22}H_{40}$	$FeP_2O_3C_{19}H_{26}$
mol wt	549	420
cryst system	triclinic	triclinic
cell parameters		
a, Å	10.640 (1)	9.822 (1)
b, Å	10.865 (2)	9.845 (1)
c, Å	24.908 (4)	10.913 (1)
α, deg	90.14 (1)	74.64 (1)
β, deg	95.06 (1)	67.02 (1)
γ, deg	112.24 (1)	80.74 (1)
V, Å^3	2653	935
space group	$P\bar{1}$	$P\bar{1}$
Z; d_{obsd}, d_{calcd}, g cm^{-3}	4; 1.37 ± 0.02, 1.375	2; 1.49 ± 0.02, 1.493
μ, cm^{-1}	151	83
$F(000)$	1124	440
θ range	$2° < \theta < 60°$	$2° < \theta < 60°$
tot. no. of measmts	5431	2354
no. of obsd reflctns ($\sigma(I)/I < 0.33$)	4115	2218
$R(F)$	0.060	0.036
$R_w(F)$	0.077	0.057
fudge factor p in $\sigma^2(F^2) = \sigma_{count}^2 + (pF^2)^2$	0.08	0.07
esd of unit wt obsd	1.42	1.43

(6) F. Mathey and R. Mankowski-Favelier, *Bull. Soc. Chim. Fr.*, 4433 (1970).
(7) F. B. Clarke III and F. H. Westheimer, *J. Am. Chem. Soc.*, **93**, 4541 (1971).
(8) D. G. Holah, A. N. Hughes, and K. Wright, *Coord. Chem. Rev.*, **15**, 239 (1975).
(9) K. Yasufuku, A. Amada, K. Aoki, and H. Yamazaki, *J. Am. Chem. Soc.*, **102**, 4363 (1980).
(10) M. J. Barrow, J. L. Davidson, W. Harrison, D. W. A. Sharp, G. A. Sim, and F. B. Wilson, *J. Chem. Soc., Chem. Commun.*, 583 (1973); M. J. Barrow, A. A. Freer, W. Harrison, G. A. Sim, D. W. Taylor, and F. B. Wilson, *J. Chem. Soc., Dalton Trans.*, 197 (1975).
(11) Drawings were done with use of the program ORTEP II: C. K. Johnson, Report ORNL 3794, Oak Ridge National Laboratory, Oak Ridge, Tenn., 1965.

Table II. Positional and Thermal Parameters and Their Estimated Standard Deviations for $FeP_2IC_{22}H_{40}$ (7)[a]

atom	x	y	z	B(1,1)	B(2,2)	B(3,3)	B(1,2)	B(1,3)	B(2,3)
I1	0.21075 (7)	0.08375 (8)	0.38242 (4)	0.01167 (8)	0.01396 (9)	0.00234 (2)	0.0107 (1)	0.00275 (7)	0.00014 (7)
I2	0.24532 (8)	0.71358 (8)	−0.10720 (3)	0.01342 (9)	0.01237 (9)	0.00157 (2)	0.0083 (1)	0.00232 (6)	0.00113 (7)
Fe1	0.3379 (2)	1.0452 (2)	−0.37601 (7)	0.0091 (2)	0.0105 (2)	0.00077 (3)	0.0071 (3)	0.0006 (1)	0.0007 (1)
Fe2	0.2957 (1)	0.8133 (2)	0.11639 (7)	0.0077 (1)	0.0105 (2)	0.00071 (3)	0.0069 (2)	0.0011 (1)	0.0004 (1)
P1	0.2766 (3)	0.8339 (3)	−0.3134 (1)	0.0089 (3)	0.0115 (3)	0.00085 (5)	0.0082 (4)	0.0016 (2)	0.0007 (2)
P2	0.5430 (3)	1.2820 (3)	−0.3839 (1)	0.0101 (3)	0.0108 (3)	0.00126 (6)	0.0071 (5)	0.0007 (2)	0.0006 (2)
P3	0.5105 (3)	0.7403 (3)	0.1139 (1)	0.0088 (3)	0.0100 (3)	0.00077 (5)	0.0072 (4)	0.0012 (2)	0.0006 (2)
P4	0.2169 (3)	0.9759 (3)	0.1741 (1)	0.0103 (3)	0.0123 (3)	0.00117 (6)	0.0095 (4)	0.0026 (2)	0.0008 (2)
C1	0.4040 (9)	0.892 (1)	−0.3582 (4)	0.0081 (10)	0.011 (1)	0.0007 (2)	0.006 (2)	0.0024 (7)	0.0027 (8)
C2	0.3362 (10)	0.876 (1)	−0.4107 (4)	0.0089 (11)	0.010 (1)	0.0006 (2)	0.003 (2)	0.0019 (8)	0.0009 (8)
C3	0.2011 (10)	0.871 (1)	−0.4112 (4)	0.0097 (11)	0.010 (1)	0.0008 (2)	0.004 (2)	−0.0015 (8)	−0.0009 (9)
C4	0.1669 (10)	0.882 (1)	−0.3573 (5)	0.0099 (11)	0.010 (1)	0.0012 (2)	0.007 (2)	−0.0002 (8)	−0.0011 (9)
C5	0.3995 (13)	0.859 (1)	−0.4613 (5)	0.0172 (15)	0.015 (2)	0.0015 (3)	0.009 (2)	0.0046 (10)	0.0003 (11)
C6	0.1023 (13)	0.848 (1)	−0.4602 (5)	0.0168 (16)	0.013 (1)	0.0016 (3)	0.009 (2)	−0.0009 (11)	−0.0015 (11)
C7	0.3211 (11)	0.920 (1)	−0.2485 (4)	0.0132 (13)	0.015 (1)	0.0007 (2)	0.008 (2)	0.0017 (9)	0.0008 (10)
C8	0.2185 (11)	0.657 (1)	−0.3007 (5)	0.0120 (12)	0.010 (1)	0.0017 (2)	0.009 (2)	0.0015 (9)	0.0025 (9)
C9	0.3360 (13)	0.630 (1)	−0.2699 (6)	0.0178 (15)	0.017 (2)	0.0023 (3)	0.019 (2)	0.0013 (12)	0.0031 (12)
C10	0.0933 (14)	0.617 (1)	−0.2688 (6)	0.0160 (17)	0.016 (2)	0.0019 (3)	−0.002 (3)	0.0036 (12)	0.0010 (13)
C11	0.1779 (13)	0.577 (1)	−0.3557 (5)	0.0196 (17)	0.015 (2)	0.0014 (3)	0.012 (3)	−0.0002 (12)	0.0012 (11)
C12	0.4050 (10)	1.197 (1)	−0.4311 (4)	0.0119 (12)	0.008 (1)	0.0008 (2)	0.006 (2)	0.0018 (8)	−0.0001 (8)
C13	0.2839 (11)	1.192 (1)	−0.4100 (4)	0.0131 (12)	0.013 (1)	0.0007 (2)	0.011 (2)	0.0005 (9)	0.0008 (9)
C14	0.2993 (11)	1.202 (1)	−0.3531 (5)	0.0123 (12)	0.010 (1)	0.0015 (2)	0.008 (2)	0.0023 (9)	0.0008 (10)
C15	0.4385 (11)	1.223 (1)	−0.3314 (4)	0.0169 (13)	0.011 (1)	0.0004 (2)	0.011 (2)	0.0023 (9)	0.0019 (8)
C16	0.1537 (11)	1.181 (1)	−0.4435 (6)	0.0107 (13)	0.018 (2)	0.0022 (3)	0.012 (2)	−0.0005 (11)	0.0022 (12)
C17	0.1919 (12)	1.204 (1)	−0.3164 (6)	0.0159 (14)	0.013 (1)	0.0020 (3)	0.010 (2)	0.0043 (10)	−0.0001 (11)
C18	0.6795 (12)	1.222 (1)	−0.3829 (6)	0.0130 (13)	0.014 (1)	0.0025 (3)	0.013 (2)	0.0025 (11)	0.0010 (12)
C19	0.6180 (11)	1.463 (1)	−0.3880 (5)	0.0130 (13)	0.009 (1)	0.0018 (3)	0.006 (2)	0.0008 (10)	0.0026 (10)
C20	0.6971 (17)	1.504 (1)	−0.4368 (7)	0.0294 (23)	0.013 (2)	0.0036 (4)	0.009 (3)	0.0120 (15)	0.0061 (14)
C21	0.5068 (14)	1.517 (1)	−0.3944 (7)	0.0208 (19)	0.014 (2)	0.0037 (4)	0.013 (3)	0.0035 (15)	0.0044 (14)
C22	0.7005 (17)	1.525 (1)	−0.3343 (8)	0.0271 (24)	0.013 (2)	0.0040 (5)	0.007 (3)	−0.0081 (17)	0.0010 (16)
C23	0.3759 (9)	0.717 (1)	0.0636 (4)	0.0064 (10)	0.012 (1)	0.0008 (2)	0.004 (2)	0.0010 (8)	0.0011 (9)
C24	0.2552 (10)	0.626 (1)	0.0850 (4)	0.0102 (11)	0.008 (1)	0.0011 (2)	0.007 (2)	0.0007 (8)	0.0004 (8)
C25	0.2666 (10)	0.629 (1)	0.1416 (5)	0.0087 (11)	0.009 (1)	0.0013 (2)	0.004 (2)	0.0020 (8)	0.0018 (9)
C26	0.3998 (10)	0.718 (1)	0.1647 (4)	0.0112 (11)	0.011 (1)	0.0007 (2)	0.008 (2)	0.0030 (8)	0.0009 (8)
C27	0.1315 (12)	0.535 (1)	0.0499 (5)	0.0118 (14)	0.014 (2)	0.0014 (3)	0.003 (2)	−0.0010 (10)	−0.0015 (11)
C28	0.1583 (12)	0.546 (1)	0.1759 (5)	0.0153 (15)	0.012 (1)	0.0018 (3)	0.006 (2)	0.0028 (11)	0.0011 (11)
C29	0.6451 (10)	0.903 (1)	0.1169 (4)	0.0082 (11)	0.014 (1)	0.0009 (2)	0.004 (2)	−0.0010 (8)	−0.0003 (10)
C30	0.5935 (11)	0.620 (1)	0.1117 (5)	0.0137 (12)	0.011 (1)	0.0016 (2)	0.013 (2)	0.0028 (9)	0.0025 (9)
C31	0.6941 (13)	0.640 (1)	0.1609 (6)	0.0186 (15)	0.021 (2)	0.0021 (3)	0.021 (2)	−0.0024 (12)	0.0015 (13)
C32	0.4829 (13)	0.480 (1)	0.1115 (7)	0.0177 (15)	0.010 (1)	0.0044 (4)	0.014 (2)	0.0061 (13)	0.0030 (13)
C33	0.6640 (13)	0.635 (1)	0.0594 (6)	0.0214 (16)	0.017 (2)	0.0028 (3)	0.021 (2)	0.0071 (12)	0.0035 (13)
C34	0.3514 (9)	1.015 (1)	0.1322 (4)	0.0063 (9)	0.011 (1)	0.0012 (2)	0.005 (2)	0.0036 (7)	0.0019 (9)
C35	0.2936 (10)	0.978 (1)	0.0790 (4)	0.0108 (10)	0.012 (1)	0.0008 (2)	0.013 (2)	0.0016 (8)	0.0006 (8)
C36	0.1573 (10)	0.878 (1)	0.0758 (4)	0.0114 (11)	0.013 (1)	0.0008 (2)	0.012 (2)	0.0004 (8)	−0.0005 (9)
C37	0.1180 (10)	0.844 (1)	0.1287 (5)	0.0094 (11)	0.011 (1)	0.0016 (2)	0.008 (2)	0.0014 (9)	0.0001 (10)
C38	0.3616 (12)	1.038 (1)	0.0305 (5)	0.0184 (15)	0.016 (1)	0.0015 (2)	0.018 (2)	0.0039 (10)	0.0040 (11)
C39	0.0684 (12)	0.821 (1)	0.0257 (6)	0.0143 (14)	0.022 (2)	0.0021 (3)	0.020 (2)	−0.0008 (11)	−0.0015 (13)
C40	0.2489 (12)	0.923 (1)	0.2391 (5)	0.0203 (15)	0.015 (1)	0.0017 (3)	0.020 (2)	0.0037 (11)	0.0023 (11)
C41	0.1530 (11)	1.109 (1)	0.1842 (5)	0.0148 (12)	0.013 (1)	0.0017 (3)	0.015 (2)	0.0035 (9)	0.0005 (10)
C42	0.0259 (12)	1.054 (1)	0.2150 (7)	0.0162 (13)	0.023 (2)	0.0036 (4)	0.024 (2)	0.0059 (12)	0.0003 (14)
C43	0.2631 (14)	1.222 (1)	0.2165 (6)	0.0222 (18)	0.012 (1)	0.0027 (4)	0.015 (2)	0.0003 (14)	−0.0014 (13)
C44	0.1198 (13)	1.152 (1)	0.1285 (6)	0.0187 (15)	0.019 (2)	0.0025 (3)	0.023 (2)	0.0012 (12)	0.0003 (13)

[a] The form of the anisotropic thermal parameter is $\exp[-(B(1,1)h^2 + B(2,2)k^2 + B(3,3)l^2 + B(1,2)hk + B(1,3)hl + B(2,3)kl)]$.

observed in the starting diphosphaferrocene **4**[5] and the phosphole rings of **7** act as η^4 ligands. No structural data are available for free phospholium salts. Nevertheless the comparison of the structure of a trivalent phosphindole with that of its methyl iodide salt[12,13] shows conclusively that the quaternization of phosphorus tends to reduce the bending of such five-membered rings. On the other hand, similar dihedral angle values ($\simeq 30°$) were observed in π complexes of phosphole esters[9] and phosphole acids[10] whereas free phosphole oxides are almost planar.[14] Thus, the very large dihedral angles observed in **7** are obviously a consequence of the η^4 complexation. Such envelope conformations have already been noted for cyclopentadiene–cobalt and –rhenium complexes[15,16] and have been ascribed to an inward twisting of the p orbitals of the α-carbons for a better overlap with the metal orbitals.

Another curious structural difference of **7** by comparison with diphosphaferrocene **4** is shown on Figure 2: the phosphorus of one ring superposes with the α-carbon of the other (superposition with the β-carbon in **4**[5]). By contrast the iron–C(ring) mean distances are remarkably similar in **7** and **4**. It is also interesting to note that both *tert*-butyls of **7** are exo; this is obviously due to their steric bulk. Finally, whereas cyclic delocalization is impossible in a phospholium ring, the intracyclic P–C bonds of **7** remain significantly shorter than

(12) W. Winter, *Chem. Ber.*, **110**, 2168 (1977).
(13) W. Winter and J. Strähle, *Chem. Ber.*, **110**, 1477 (1977).
(14) M. Dräger and K. G. Walter, *Chem. Ber.*, **109**, 877 (1976).
(15) M. R. Churchill, *J. Organomet. Chem.*, **4**, 258 (1965).
(16) N. W. Alcock, *J. Chem. Soc. A*, 2001 (1967).
(17) S. C. Abrahams and J. L. Bernstein, *J. Chem. Phys.*, **44**, 2223 (1966).
(18) F. Mathey, *Tetrahedron*, **28**, 4171 (1972).
(19) B. A. Frenz in "Computing in Crystallography", H. Schenk, R. Olthof-Hazekamp, H. Van Koenigsveld, and G. C. Bassi, Eds., Delft University Press, Delft, Holland, 1978, p 64.
(20) "International Tables for X-ray Crystallography", Vol. II, Kynoch Press, Birmingham, England, 1959, p 302.
(21) G. Germain, P. Main, and M. H. Woolfson, *Acta Crystallogr., Sect. B*, **B26**, 274 (1970); *Acta Crystallogr., Sect. A*, **A27**, 368 (1971).

Table III. Positional and Thermal Parameters and Their Estimated Standard Deviations for $FeP_2O_3C_{19}H_{26}$ (14)[a]

atom	x	y	z	B(1,1)	B(2,2)	B(3,3)	B(1,2)	B(1,3)	B(2,3)
Fe	0.87653 (5)	0.30239 (5)	0.24812 (4)	0.00537 (5)	0.00521 (5)	0.00503 (4)	−0.00114 (8)	−0.00377 (7)	−0.00285 (7)
P1	1.13788 (8)	0.14209 (9)	0.21023 (8)	0.00584 (8)	0.00692 (9)	0.00670 (7)	−0.0004 (1)	−0.0048 (1)	−0.0032 (1)
P2	0.86290 (9)	0.54596 (9)	0.25396 (8)	0.00866 (9)	0.00601 (8)	0.00751 (7)	−0.0013 (1)	−0.0062 (1)	−0.0046 (1)
O1	1.0102 (2)	0.4582 (2)	0.2425 (2)	0.0083 (2)	0.0073 (2)	0.0095 (2)	−0.0020 (4)	−0.0084 (3)	−0.0050 (4)
O2	0.8578 (3)	0.6959 (3)	0.2583 (3)	0.0147 (3)	0.0071 (3)	0.0128 (3)	−0.0015 (5)	−0.0104 (4)	−0.0074 (4)
O3	0.1448 (4)	0.3566 (5)	0.4545 (3)	0.0186 (4)	0.0294 (6)	0.0169 (3)	0.0001 (9)	−0.0170 (6)	−0.0179 (7)
C1	0.9755 (3)	0.1411 (3)	0.3581 (3)	0.0071 (3)	0.0067 (3)	0.0063 (3)	−0.0005 (6)	−0.0044 (5)	−0.0038 (5)
C2	0.8618 (3)	0.0915 (3)	0.3330 (3)	0.0065 (3)	0.0052 (3)	0.0079 (3)	−0.0005 (6)	−0.0039 (5)	−0.0020 (5)
C3	0.8916 (3)	0.1177 (3)	0.1895 (3)	0.0071 (3)	0.0058 (3)	0.0082 (3)	0.0008 (6)	−0.0071 (5)	−0.0046 (5)
C4	1.0277 (3)	0.1852 (3)	0.1099 (3)	0.0074 (3)	0.0063 (3)	0.0063 (3)	0.0009 (6)	−0.0052 (5)	−0.0038 (5)
C5	0.7386 (4)	0.0087 (4)	0.4425 (4)	0.0097 (4)	0.0085 (4)	0.0105 (4)	−0.0041 (7)	−0.0049 (7)	0.0020 (7)
C6	0.8049 (4)	0.0613 (4)	0.1299 (4)	0.0123 (4)	0.0084 (4)	0.0132 (3)	0.0012 (7)	−0.0146 (5)	−0.0099 (6)
C7	1.2708 (4)	0.2666 (4)	0.1694 (4)	0.0065 (4)	0.0101 (4)	0.0109 (4)	−0.0033 (7)	−0.0051 (6)	−0.0047 (6)
C8	1.2417 (4)	−0.0297 (4)	0.2109 (3)	0.0079 (4)	0.0089 (4)	0.0063 (3)	0.0031 (7)	−0.0054 (5)	−0.0042 (6)
C9	1.3925 (4)	−0.0467 (4)	0.1887 (4)	0.0087 (4)	0.0121 (5)	0.0116 (4)	0.0043 (8)	−0.0071 (6)	−0.0070 (7)
C10	1.4641 (4)	−0.1791 (5)	0.1987 (4)	0.0101 (5)	0.0166 (6)	0.0131 (4)	0.0115 (9)	−0.0083 (7)	−0.0121 (8)
C11	1.3871 (5)	−0.2950 (5)	0.2282 (4)	0.0168 (6)	0.0120 (5)	0.0102 (4)	0.0139 (9)	−0.0095 (7)	−0.0071 (8)
C12	1.2381 (5)	−0.2808 (4)	0.2475 (4)	0.0178 (6)	0.0086 (5)	0.0096 (4)	0.0038 (9)	−0.0056 (8)	−0.0047 (7)
C13	1.1664 (4)	−0.1480 (4)	0.2389 (4)	0.0101 (4)	0.0083 (4)	0.0088 (3)	0.0025 (7)	−0.0054 (6)	−0.0045 (6)
C14	0.8202 (3)	0.4921 (3)	0.1288 (3)	0.0076 (3)	0.0065 (4)	0.0060 (3)	0.0005 (6)	−0.0053 (5)	−0.0027 (5)
C15	0.6981 (3)	0.4097 (3)	0.1881 (3)	0.0067 (3)	0.0068 (4)	0.0084 (3)	0.0009 (6)	−0.0070 (5)	−0.0047 (5)
C16	0.6485 (3)	0.3719 (3)	0.3349 (3)	0.0057 (3)	0.0063 (4)	0.0079 (3)	0.0015 (6)	−0.0015 (5)	−0.0038 (6)
C17	0.7344 (4)	0.4262 (4)	0.3851 (3)	0.0094 (4)	0.0070 (4)	0.0063 (3)	0.0008 (7)	−0.0036 (5)	−0.0050 (5)
C18	0.6239 (4)	0.3728 (4)	0.1058 (4)	0.0107 (4)	0.0108 (5)	0.0137 (4)	0.0019 (7)	−0.0157 (5)	−0.0075 (7)
C19	0.5120 (4)	0.2944 (4)	0.4232 (4)	0.0068 (4)	0.0108 (5)	0.0119 (5)	−0.0014 (8)	−0.0007 (7)	−0.0020 (8)

[a] The form of the anisotropic thermal parameter is $\exp[-(B(1,1)h^2 + B(2,2)k^2 + B(3,3)l^2 + B(1,2)hk + B(1,3)hl + B(2,3)kl)]$.

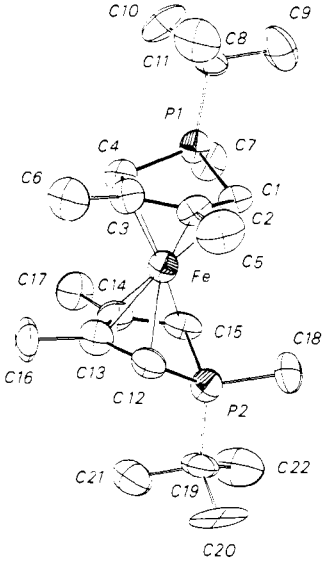

Figure 1. ORTEP view of 7 molecule I, together with the labeling scheme used. Molecule II contains atoms labeled Fe2, P3, P4, and carbon atoms C23–C44. Atoms are represented by their thermal motion ellipsoids scaled to enclose 50% of the electron density, and hydrogen atoms are omitted.

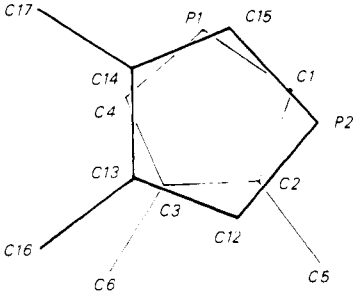

Figure 2. Projection of 7, molecule I, on the plane defined by atoms C1–C4.

the exocyclic ones; this is probably another consequence of the η^4 complexation.

Table IV. Contacts Less Than 3 Å for 7

A	B	dist[a]	
H1C9	H1C31	2.81	$\bar{1}$/110
H1C9	H3C31	2.60	$\bar{1}$/110
H2C9	H3C21	2.71	1/0$\bar{1}$0
H1C10	H1C28	2.80	$\bar{1}$/010
H1C10	H2C28	2.79	$\bar{1}$/010
H3C10	H1C22	2.97	1/$\bar{1}\bar{1}$0
H3C10	H3C22	2.53	1/$\bar{1}\bar{1}$0
H3C11	H3C21	2.72	1/0$\bar{1}$0
H1C27	H1C27	2.87	$\bar{1}$/010
H1C27	H3C27	2.47	$\bar{1}$/010
H2C27	HAC39	2.92	$\bar{1}$/010
H2C27	H3C39	2.91	$\bar{1}$/010
H2C27	H1C44	2.97	1/0$\bar{1}$0
H3C27	H3C27	2.97	$\bar{1}$/010
H3C28	H1C43	2.66	1/0$\bar{1}$0
H3C28	H1C44	2.52	1/0$\bar{1}$0
H2C29	H2C42	2.59	1/100
H2C31	H2C42	2.78	1/100
H2C32	H3C43	2.61	1/0$\bar{1}$0
H3C32	H2C33	2.86	$\bar{1}$/110
H1C33	H1C39	2.94	1/100
H2C33	H2C33	2.88	$\bar{1}$/110
H3C33	H1C39	2.68	1/100

[a] The relative coordinates of the atoms in column A are listed in Table VIII. The atoms in column B have their atomic parameters specified by *I/uvw*, which denotes how the parameters can be derived from the corresponding atoms in the following crystal units: (1) x, y, z; (−1) $\bar{x}, \bar{y}, \bar{z}$. The u, v, and w code a lattice translation as $ua + vb + wc$.

14. As for **7**, the crystal structure of $[(CH_3)_2C_4H_2P(CH_3)(C_6H_5)][(CH_3)_2C_4H_2PO_2]Fe{\cdot}H_2O$ consists of discrete molecules in which the iron atom is sandwiched between π-bonded rings, phosphole ring number one with a phenyl and a methyl group bonded to the P atom and ring number two with two oxygen atoms bonded to P. Individual molecules are linked by hydrogen bonds and van der Waals type interactions as shown in Table VII. A water molecule connects two molecules together, and the oxygen atom O2 is linked via hydrogen bonds to a third molecule. Figure 3 gives a view of the molecule.

Table V. Selected Bond Lengths (Å) and Angles (Deg) with Averages and Esd's for 7

molecule I		molecule II		averages	
Fe1-P1	2.682 (3)	Fe2-P3	2.694 (3)		
Fe1-P2	2.692 (3)	Fe2-P4	2.686 (3)	Fe-P	2.688 (1)
Fe1-C1	2.07 (1)	Fe2-C23	2.10 (1)		
Fe1-C2	2.02 (1)	Fe2-C24	2.05 (1)		
Fe1-C3	2.03 (1)	Fe2-C25	2.01 (1)		
Fe1-C4	2.09 (1)	Fe2-C26	2.09 (1)		
Fe1-C12	2.10 (1)	Fe2-C34	2.07 (1)		
Fe1-C13	2.05 (1)	Fe2-C35	2.03 (1)		
Fe1-C14	1.99 (1)	Fe2-C36	2.05 (1)		
Fe1-C15	2.08 (1)	Fe2-C37	2.08 (1)	Fe-C	2.059 (2)
P1-C1	1.76 (1)	P3-C23	1.75 (1)		
P1-C4	1.75 (1)	P3-C26	1.76 (1)		
P2-C12	1.75 (1)	P4-C34	1.76 (1)		
P2-C15	1.75 (1)	P4-C37	1.75 (1)	P-C	1.757 (3)
P1-C7	1.80 (1)	P3-C29	1.80 (1)		
P2-C18	1.80 (1)	P4-C40	1.77 (1)	P-C(Me)	1.791 (5)
P1-C8	1.82 (1)	P3-C30	1.83 (1)		
P2-C19	1.83 (1)	P4-C41	1.84 (1)	P-C(*t*-Bu)	1.832 (5)
C1-C2	1.41 (1)	C23-C24	1.44 (1)		
C2-C3	1.41 (1)	C24-C25	1.40 (1)		
C3-C4	1.44 (1)	C25-C26	1.44 (1)		
C12-C13	1.41 (1)	C34-C35	1.40 (3)		
C13-C14	1.41 (1)	C35-C36	1.44 (1)		
C14-C15	1.46 (1)	C36-C37	1.42 (1)	C-C	1.426 (4)
C2-C5	1.52 (1)	C24-C27	1.51 (1)		
C3-C6	1.49 (1)	C25-C28	1.50 (1)		
C13-C16	1.52 (1)	C35-C38	1.48 (1)		
C14-C17	1.53 (1)	C36-C39	1.47 (1)	C-C(Me)	1.505 (5)
C8-C9	1.52 (1)	C30-C31	1.51 (1)		
C8-C10	1.53 (1)	C30-C32	1.53 (1)		
C8-C11	1.55 (1)	C30-C33	1.54 (1)		
C19-C20	1.51 (1)	C41-C42	1.53 (1)		
C19-C21	1.50 (1)	C41-C43	1.50 (1)		
C19-C22	1.53 (1)	C41-C44	1.52 (1)	C-C(*t*-Bu)	1.525 (4)
C1-P1-C4	90.1 (4)	C23-P3-C26	90.9 (4)		
C12-P2-C15	90.0 (5)	C34-P4-C37	89.0 (5)	C-P-C	90.0 (2)
C1-P1-C7	114.4 (4)	C23-P3-C29	114.8 (4)		
C4-P1-C7	114.2 (5)	C26-P3-C29	113.5 (5)		
C12-P2-C18	113.8 (5)	C34-P4-C40	116.0 (5)		
C15-P2-C18	113.5 (5)	C37-P4-C40	113.1 (5)	C-P-C(Me)	114.1 (2)
C1-P1-C8	115.1 (5)	C23-P3-C30	115.7 (5)		
C4-P1-C8	115.8 (5)	C26-P3-C30	115.4 (5)		
C12-P2-C19	116.2 (5)	C34-P4-C41	115.0 (5)		
C15-P2-C19	115.2 (5)	C37-P4-C41	117.2 (5)	C-P-C(*t*-Bu)	115.8 (2)
C7-P1-C8	106.7 (5)	C29-P3-C30	106.2 (5)		
C18-P2-C19	107.5 (5)	C40-P4-C41	106.2 (5)	C(Me)-P-C(*t*-Bu)	106.6 (2)
C1-C2-C3	113.3 (8)	C23-C24-C25	112.6 (8)		
C2-C3-C4	110.8 (8)	C24-C25-C26	112.2 (8)		
C12-C13-C14	111.7 (8)	C34-C35-C36	112.8 (8)		
C13-C14-C15	111.6 (8)	C35-C36-C37	109.9 (8)	C-C-C	111.9 (2)
P1-C1-C2	106.8 (6)	P3-C23-C24	105.8 (7)		
P1-C4-C3	107.4 (7)	P2-C26-C25	106.5 (6)		
P2-C12-C13	108.4 (7)	P4-C34-C35	107.9 (6)		
P2-C15-C14	107.1 (7)	P4-C37-C36	108.7 (7)	P-C-C	107.3 (2)

Table VIII gives selected bond lengths and angles and Table IX the least-squares planes of interest.

The phospholium ring of **14** is geometrically very similar to the rings of **7**; the dihedral angle between mean planes PL_1 and PL_2 is just slightly larger (34.3° vs. 30.9°) and, consequently, the Fe–P_1 bond length is longer (2.732 (1) Å vs. 2.688 (1) Å). Quite logically, the phenyl substituent is exo. By contrast, the other ring of **14** has a very different geometry. It acts as a chelating ligand since O_1 is bonded to iron. This bonding causes a drastic decrease of the PL_3–PL_4 dihedral angle down to 10.4° (see Table VI), which, in turn, reduces the overlap of the *p* orbitals of the α carbons with the metal orbitals. Thus, the C_{14}–C_{15}–C_{16}–C_{17} diene is less strongly coordinated to the iron atom than the C_1–C_2–C_3–C_4 diene (Fe–(diene plane) distance 1.682 (0) Å vs. 1.645 (0) Å). As a consequence the C_{14}–C_{15} and C_{16}–C_{17} bonds acquire a more pronounced double-bond character (mean value 1.396 Å vs. 1.441 Å for C_{15}–C_{16}). Such a phenomenon is not seen in η^4-complexed phosphole esters[9] and phosphole acids[10] but has been already noted to a lesser extent in previously described η^1,η^4-phosphole complexes.[22]

Two possible limit forms can be written for the $FePO_2$ unit of **14**: Fe^-—O_1—P_2=O_2 or Fe←O_1=P_2—O_2^-. The observed distances, Fe–O_1 = 2.148 (2) Å, O_1–P_2 = 1.539 (2) Å, and P_2–O_2 = 1.482 (2) Å, are very similar to those observed in $Fe_3(PO_4)_2{\cdot}4H_2O$,[17] Fe–O (mean) = 2.14 and 2.17 Å and P–O (mean) = 1.542 Å, on one side, and to that observed in a η^4-complexed phosphole ester,[9] P=O = 1.484 (3) Å, on the other side. Hence **14** must be considered as a iron phosphinate in which the phosphole acid acts as a five-electron ligand and where iron bears a formal negative charge, and not as a phosphoryl–iron coordination complex. Finally it is interesting to note that the respective orientation of the two phosphole

(22) J. M. Rosalky, B. Metz, F. Mathey, and R. Weiss, *Inorg. Chem.*, **16**, 3307 (1977).

Table VI. Mean Least-Squares Planes for 7

plane	atoms in plane	equation *a*	*b*	*c*	*d*	χ^2	dist to plane, Å
PL1	C1, C2, C3, C4	−0.0387	0.9975	−0.0597	9.7620	0	Fe1 1.636 (2), P1 −0.640 (3), C5 −0.088 (13), C6 −0.078 (12)
PL2	P1, C1, C4	0.0303	−0.8854	−0.4639	−4.0825	0	
PL3	C12, C13, C14, C15	−0.1011	0.9932	−0.0578	12.9652	6	Fe1 −1.639 (2), P2 0.621 (3), C16 0.124 (13), C17 0.038 (12)
PL4	P2, C12, C15	−0.5869	0.8083	−0.0466	10.3722	0	
PL5	C23, C24, C25, C26	0.6758	−0.7366	−0.0264	−4.6796	7	Fe2 −1.645 (2), P3 0.647 (3), C27 0.107 (13), C28 0.003 (13)
PL6	P3, C23, C26	0.1885	−0.9814	−0.0370	−6.9004	0	
PL7	C34, C35, C36, C37	0.6975	−0.7166	−0.0085	−7.7604	0	Fe2 1.639 (2), P4 −0.645 (3), C38 −0.048 (13), C39 −0.032 (14)
PL8	P4, C34, C37	−0.5889	0.6302	−0.5060	5.1247	0	
PL9	P1, C7, C8, Fe1	−0.9993	−0.0380	−0.0013	−0.5243	2	C1 −1.236 (11), C4 1.251 (12), C2 −0.687 (11), C3 0.728 (12), C5 −1.537 (15), C6 1.586 (15), C9 −1.293 (14), C10, 1.239 (16), C11 0.002 (15)
PL10	P2, C18, C19, Fe1	−0.0194	−0.0698	−0.9974	8.5366	5	C12 1.248 (11), C15 −1.229 (10), C13 0.757 (11), C14 −0.654 (12), C16 1.614 (14), C17 −1.536 (14), C20 1.136 (17), C21 0.125 (18), C22 −1.401 (19)
PL11	P3, C29, C30, Fe2	−0.0105	0.0456	−0.9989	−2.5091	2	C23 1.250 (11), C26 −1.256 (10), C24 0.689 (11), C25 −0.715 (11), C27 1.526 (13), C28 −1.593 (13), C31 −1.236 (13), C32 −0.068 (17), C33 1.280 (16)
PL12	P4, C40, C41, Fe2	−0.7263	−0.6836	−0.0726	−5.3935	3	C34 −1.209 (11), C37 1.260 (1), C35 −0.642 (11), C36 0.797 (1), C38 −1.423 (13), C39 1.684 (1), C42 1.195 (14), C43 −1.291 (1), C44 0.048 (14)

dihedral angles: PL1/PL2, 31.1; PL3/PL4, 30.1; PL5/PL6, 31.7; PL7/PL8, 30.9; PL1/PL3, 3.6; PL5/PL7, 2.0

Table VII. Contacts Less Than 3 Å for 14[a]

A	B	dist	
O1	H12	2.78	1/010
O2	H13	2.77	1/010
O2	H62	2.60	1/$\bar{0}$10
O3	H72	2.71	1/$\bar{1}$00
H9	H63	2.65	1/1$\bar{0}$0
H11	H183	2.44	1/1$\bar{1}$0
H11	H192	2.77	1/1$\bar{1}$0
H72	H183	2.53	1/100
H73	H183	2.70	1/100

[a] See footnote for Table IV.

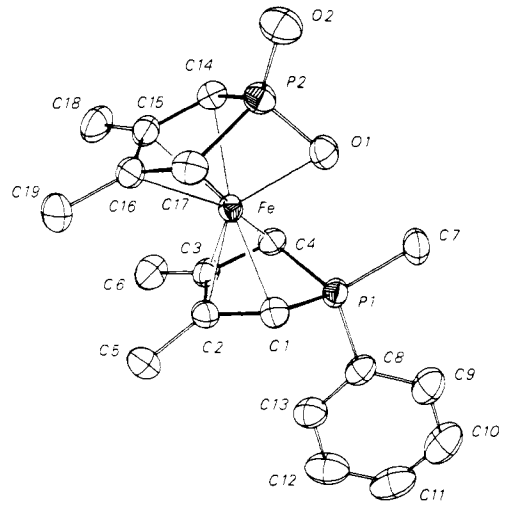

Figure 3. ORTEP view of **14** together with the labeling scheme used. Atoms are represented by their thermal motion ellipsoids scaled to enclose 50% of the electron density, and hydrogen atoms are omitted.

rings has again changed when passing from **7** to **14**; in **14**, the two phosphorus atoms are now one under the other.

Experimental Section

NMR spectra [chemical shifts in ppm from internal Me_4Si for ^1H and from H_3PO_4 (external reference) for ^{31}P; δ positive for downfield shifts in all cases] were recorded for the proton resonances on a Perkin-Elmer R 24A at 60 MHz and for the phosphorus resonances on a Bruker WH-90 at 36.412 MHz. All reactions were carried out under argon. Chromatographic separations were performed on silica gel columns (70–230 mesh Merck).

Table VIII. Selected Bond Lengths (Å) and Angles (Deg) for 14

Fe–P1	2.732 (1)	C1–C2	1.430 (4)
Fe–P2	2.396 (1)	C2–C3	1.434 (4)
Fe–C1	2.076 (3)	C3–C4	1.434 (4)
Fe–C2	2.040 (3)	C14–C15	1.394 (4)
Fe–C3	2.047 (3)	C15–C16	1.441 (4)
Fe–C4	2.105 (3)	C16–C17	1.399 (4)
Fe–C14	2.106 (3)	C2–C5	1.493 (4)
Fe–C15	2.133 (3)	C3–C6	1.495 (4)
Fe–C17	2.111 (3)	C15–C18	1.497 (4)
Fe–O1	2.148 (2)	C16–C19	1.497 (4)
P1–C1	1.771 (3)	C8–C9	1.393 (5)
P1–C4	1.755 (3)	C9–C10	1.377 (5)
P2–C14	1.796 (3)	C10–C11	1.367 (6)
P2–C17	1.791 (3)	C11–C12	1.383 (6)
P1–C7	1.783 (3)	C12–C13	1.380 (5)
P1–C8	1.829 (3)	C13–C8	1.381 (5)
P2–O1	1.539 (2)		
P2–O2	1.482 (2)		

C1–P1–C4	89.4 (1)	P1–C1–C2	106.8 (2)
C1–P1–C7	118.5 (1)	P1–C4–C3	106.9 (2)
C4–P1–C7	114.6 (1)	P2–C14–C15	112.1 (2)
C1–P1–C8	112.7 (1)	P2–C17–C16	112.2 (2)
C4–P1–C8	116.1 (1)	C14–P2–C17	89.1 (1)
C7–P1–C8	105.5 (1)	O1–P2–O2	117.0 (1)
C1–C2–C3	111.2 (2)	C14–P2–O1	99.6 (1)
C2–C3–C4	111.7 (2)	C17–P2–O1	100.5 (1)
C14–C15–C16	112.7 (2)	C14–P2–O2	122.8 (1)
C15–C16–C17	112.5 (2)	C17–P2–O2	122.0 (1)

Bis(η^4-1-*tert*-butyl-1,3,4-trimethylphospholium)iron Iodide (7). A stirred solution of 3,3′,4,4′-tetramethyl-1,1′-diphosphaferrocene (**4**)[5] (1 g, 3.6×10^{-3} mol) in THF (50 mL) is treated at −80 °C by 7.2 $\times 10^{-3}$ mol of *t*-BuLi in pentane. After 15 min, 2 g of methyl iodide (14.1×10^{-3} mol) is added to the solution. Then, after 0.5 h, the reaction medium is hydrolyzed with water (10 mL) at low temperature. The resulting mixture is extracted at room temperature by ethyl

Table IX. Mean Least-Squares Planes for 14

plane	equation	χ^2	dist to plane, Å
PL1	$0.3833x - 0.9232y - 0.0284z - 2.2406 = 0$	1	C1 −0.001 (3), C2 0.003 (3), C3 −0.002 (3), C4 0.001 (3), P1 0.706 (1), Fe −1.645 (0)
PL2	$0.1922x - 0.9774y - 0.0879z - 3.9906 = 0$	0	C1, C4, P1 in plane; C7 1.384 (4), C8 −1.487 (4), Fe 1.159 (0)
PL3	$0.5053x - 0.8613y - 0.0523z - 0.3097 = 0$	0	C14 −0.001 (3), C15 0.001 (3), C16 −0.001 (4), C17 0.001 (4), P2 −0.231 (1), Fe 1.682 (0)
PL4	$0.6527x - 0.7553y - 0.0584z - 2.2223 = 0$	0	C14, C17, P2 in plane; O1 1.492 (2), O2 −0.976 (3), Fe 1.620 (0)
PL5	$-0.1641x - 0.1353y - 0.9771z + 4.1760 = 0$	21	C8 −0.008 (3), C9 0.010 (4), C10 −0.002 (4), C11 −0.008 (4), C12 0.006 (4), C13 0.003 (4)

dihedral angles: PL1/PL2, 34.3°; PL3/PL4, 10.4°; PL1/PL3, 8.0°

acetate. The upper green organic layer is evaporated. The residue is chromatographed with EtOH ($R_f \sim 0.7$–0.8). Complex **7** is obtained as a green powder in 40–55% yield (0.8–1.1 g) and can be crystallized by very slow evaporation of a THF solution under argon; mp 206 °C dec. Anal. Calcd for $C_{22}H_{40}FeIP_2$: C, 48.11; H, 7.34; Fe, 10.17. Found: C, 47.51; H, 7.31; Fe, 9.46. Mass spectrum (70 eV, 200 °C): *m/e* 422 (*I* = 6%, M − I), 350 (*I* = 15%, 422 − *t*-Bu − Me), 293 (*I* = 26%, 350 − *t*-Bu), 278 (*I* = 51%, 293 − Me), 111 (*I* = 100%, 3,4-dimethylphospholyl).

It is very interesting to note that the decomposition of **7** in the spectrometer gives the starting diphosphaferrocene **4** (*m/e* 278). This gives some support to the postulated spontaneous decomposition of **6** into **4**.

The other complexes **9**, **10**, and **13** are made in the same way as **7**. They are characterized by their phospholium decomposition products in acidic $CDCl_3$ and by their mass spectra. The yield of **9** is ~20%; the $\delta(^{31}P)$ of the corresponding phospholium is 37.5. The mass spectrum (70 eV, 170 °C) is very similar to that of **7**: *m/e* 422 (*I* = 5%), 350 (*I* = 50%), 293 (*I* = 40%), 278 (*I* = 100%). The yield of **10** (very unstable) is ~10%; the $\delta(^{31}P)$ of the corresponding phospholium is 31.8 (authentic sample, 32.2). The mass spectrum showed decomposition. The yield of **13** is ~30%; $\delta(^{31}P)$ of the corresponding phospholium is 56.6. The mass spectrum showed decomposition.

Reaction of 7 with Aqueous IH. To a water solution of **7** is added an aqueous IH solution until the green color of **7** has completely disappeared. The mixture is then stirred for 1 h, and the phospholium salt **8** is extracted from water by chloroform. It can be recrystallized in THF–H_2O; yield 65%. The product thus obtained is strictly identical with the phospholium salt obtained by quaternization of 1-*tert*-butyl-3,4-dimethylphosphole by methyl iodide;[18] $\delta^{31}P(8) = 51.1$ ppm.

(η^4-1-Phenyl-1,3,4-trimethylphospholium)(1-hydroxy-1-oxo-3,4-dimethylphospholato-(2,3,4,5,*O*-η))iron (14). A stirred solution of **4** (1 g, 3.6×10^{-3} mol) in THF (50 mL) is treated at −80 °C by 3.6 $\times 10^{-3}$ mol of PhLi in ether (made from diphenylmercury and lithium). After 15 min, 1 g of methyl iodide (7×10^{-3} mol) is added to the solution. Then after 0.5 h, the reaction medium is hydrolyzed with water (10 mL) at low temperature. The resulting mixture is extracted at room temperature by ethyl acetate. The upper red organic layer is evaporated. The residue is chromatographed with EtOH ($R_f \sim 0.5$–0.6). Complex **14** is obtained as a red solid in ca. 50% yield (0.7–0.8 g) and can be crystallized with one H_2O in ethyl acetate–pentane; mp 188 °C dec. Anal. Calcd for $C_{19}H_{26}FeO_3P_2$: C, 54.31; H, 6.24; Fe, 13.29. Found: C, 54.51; H, 6.11; Fe, 13.33. ^1H NMR ($CDCl_3$): δ 1.60 (s, Me–C), 1.68 (s, Me–C), 2.37 (d, J_{H-P} = 25 Hz, CH–P), 2.85 (d, J_{H-P} = 14 Hz, Me–P^+), 3.56 (d, J_{H-P} = 18 Hz, CH–P), 7.35 (m, Ph).

Reaction of 14 with Aqueous IH. To a water suspension of **14** is added an aqueous IH solution until complete dissolution. The phospholium salt **15** is extracted from the water solution by chloroform and is characterized by ^1H and ^{31}P NMR; $\delta^{31}P(15) = 29.8$ ($CDCl_3$). The water phase is then saturated with NaCl and reextracted with $CHCl_3$. Another unstable product (probably the phosphonic acid **17**) is thus obtained; $\delta(^{31}P) = +49.5$ ($CDCl_3$).

X-ray Data Collection and Processing

Suitable single crystals for both compounds **7** and **14** were obtained as described above.

Precession photographs and a systematic search in reciprocal space using a Philips PW1100/16 automatic diffractometer show that both crystals belong to the triclinic system.

The precise unit-cell parameters and their standard deviations were obtained at room temperature with Cu Kα radiation (λ = 1.5418 Å) with use of 25 carefully selected reflections on a Enraf-Nonius CAD4F automatic diffractometer and standard software. Experimental densities were measured by flotation in a mixture of cyclohexane and methyl iodide. The results are summarized in Table I.

All quantitative diffraction data have been measured on a CAD4F automatic diffractometer controlled by a PDP 8/A computer using standard software and nickel-filtered Cu Kα radiation. For **7** a single crystal of dimensions 0.32 × 0.28 × 0.20 mm was used and for **14** a sphere of diameter 0.34 ± 0.01 mm was shaped. Table I gives details of data collection parameters used for both compounds.

The resulting data sets were transferred to a PDP11/60 computer, and for all subsequent computations the Enraf-Nonius SDPV16 package[19] was used.

Intensities were corrected for Lorentz, polarization, and absorption factors, the latter being computed from ψ-scan data of 4 reflections for **7** and by interpolation in the transmission curve for spheres[20] for **14**. For both compounds, the intensities of three reflections were monitored during data collection periods at intervals of 2 h; no decay occurred for **14**, but the crystal of **7** lost 12% of the original intensity, and linear decay corrections were applied.

Finally equivalent reflections were sorted; all reflections having $I < 3\sigma(I)$ were considered as unobserved.

Both structures were solved with direct methods using MULTAN.[21] The statistical distribution of *E* values in reciprocal space excluded the noncentrosymmetric space group *P*1. All nonhydrogen atoms could be located in the *E* maps computed with the phases of the most probable sets of MULTAN. Hydrogen atoms were introduced in structure factor calculations with their computed coordinates (C–H = 0.95 Å) and isotropic temperature factors but not refined. Table I gives the final results after full-matrix refinements, with anisotropic temperature factors for all nonhydrogen atoms, had converged. The final difference maps showed no significant maximum.

Registry No. **4**, 67887-86-9; **7**, 78549-84-5; **8**, 38066-27-2; **9**, 78549-85-6; **10**, 78529-72-3; **13**, 78529-73-4; **14**, 78529-71-2; **15**, 30540-38-6; *t*-BuLi, 594-19-4; *n*-BuLi, 109-72-8; MeLi, 917-54-4; PhLi, 591-51-5.

Supplementary Material Available: Listings of structure factor amplitudes (F_o and $F_c \times 10$) (Table X for **7** and Table XI for **14**) (28 pages). Ordering information is given on any current masthead page.